Near-Field Wideband Beamforming for RIS Based on Fresnel Zone

Qiumo Yu*, Linglong Dai*, Fellow, IEEE, and Mengnan Jian[†]

*Department of Electronic Engineering, Tsinghua University,
Beijing National Research Center for Information Science and Technology (BNRist), Beijing 100084, China

†State Key Laboratory of Mobile Network and Mobile Multimedia Technology, Shenzhen 518055, China

Wireless Research Institute, ZTE Corporation, Beijing 100029, China

Email: yqm22@mails.tsinghua.edu.cn, daill@tsinghua.edu.cn, jian.mengnan@zte.com.cn

Abstract—Reconfigurable intelligent surface (RIS) emerged as a promising solution to overcome the challenges of high path loss and easy signal blockage in millimeter-wave (mmWave) and terahertz (THz) communication systems. With the increase of RIS aperture and system bandwidth, the near-field beam split effect emerges, which causes beams at different frequencies to focus on distinct physical locations, leading to a significant gain loss of beamforming. To address this problem, we leverage the property of Fresnel zone that the beam split disappears for RIS elements along a single Fresnel zone and propose beamforming design on the two dimensions of along and across the Fresnel zones. The phase shift of RIS elements along the same Fresnel zone are designed aligned, so that the signal reflected by these element can add up in-phase at the receiver regardless of the frequency. Then the expression of equivalent channel is simplified to the Fourier transform of reflective intensity across Fresnel zones modulated by the designed phase. Based on this relationship, we prove that the uniformly distributed in-band gain with aligned phase along the Fresnel zone leads to the upper bound of achievable rate. Finally, we design phase shifts of RIS to approach this upper bound by adopting the stationary phase method. Simulation results validate the effectiveness of our proposed Fresnel zone-based method in mitigating the near-field beam split effect.

Index Terms—Reconfigurable intelligent surface (RIS), terahertz (THz) communications, millimeter-wave (mmWave) communications, near-field, beam split, Fresnel zone.

I. INTRODUCTION

With the emergence of new applications such as virtual reality, holographic images, and digital twins, communications have put forward requirements for high transmission rates [1]. Emerging technologies such as millimeter-wave (mmWave) and terahertz (THz) communications are expected to be adopted in the future, offering ultra-wide bandwidth of several gigahertz (GHz) or even higher to facilitate highspeed data transmission. However, mmWave and THz signals are easily blocked by objects in their propagation path, resulting in limited coverage range. The recent development of reconfigurable intelligent surfaces (RIS) presents a solution to the blockage issue, as it can provide an additional reflection link by beamforming [2]. Meanwhile, high path loss poses a challenge for mmWave and THz techniques [3], necessitating high beamforming gain to mitigate the loss. Thanks to its simple structure and low hardware cost, RIS usually consists

of extremely large number of elements (2304 elements [4], for example) to achieve high beamforming gain [5].

As the scale of RIS continues to increase, the future RIS-enabled wideband communication systems will work in near-field wideband scenario, facing issue on near-field beam split, which draws challenges for the system design, especially for RIS beamforming. In near-field wideband systems, due to the mismatch of frequency-dependent channel and frequency-independent phase shift of RIS, beams of different frequencies in near-field wideband systems are focused on different physical areas in the 3-dimensional space [6]. This effect, termed as near-field beam split, causes the beams deviating from the area where the user is located, seriously affecting the energy received by the user [7]. Further, authors in [8] show that near-field beam split can affect the receiving power even in the bore sight direction where no far-field beam split effect occurs.

Although many work on the issue of beam split have arisen, only very few recent publications investigated the near-field beam split of RIS. An intuitive solution is to adopt frequency-dependent modules, like true time delay (TTD) and delay adjustable metasurface (DAM), to adjust the frequency-dependent channel. A joint design of phase shifts and delay of the DAM was proposed in [9] to focus the beam of all frequency to the user's location, eliminating the gain loss caused by beam split effectively. To reduce the number of high-cost time delay unit, a sub-connected TTD architecture was proposed in [10], where an end-to-end optimization for beamforming is realized using neural network. However, the TTD-based architectures is not practical for RIS, due to the high insertion loss and unbearable complex structure [11].

An alternative way to address the near-beam split is to form wideband beam with acceptable gain in the whole frequency band. researchers in [12] partitioned the RIS into $N_{\rm sub}$ virtual subarrays (VSA), configuring each subarray to focus its beam at the user's location at different frequencies. This approach aims to achieve relatively stable gain across all subcarriers, but the gain of each subarray is limited to $1/N_{\rm sub}^2$ compared to the entire RIS since the beamforming gain is proportional to the square of the number of RIS elements [13]. Therefore, the separate beamforming design on subarrays can not get the benefit of the whole RIS plane, resulting in severe gain loss. Hence, an effective and practical beamforming method

is required to deal with the near-field beam split effect of RIS.

In this work, a near-field wideband RIS beamforming method based on Fresnel zone is proposed to address the issue of near-field beam split without extra hardware. Fresnel zones refer to the concentric ellipsoids whose focus points are the transmitter and receiver. We discover that the beam split effect disappears if RIS elements along a signal Fresnel zone are considered and the phase of the cascaded channel via these elements remains aligned regardless of frequency. Thus, we reorient the coordinate system to the two dimensions of along and across the Fresnel zones. Along the Fresnel zone, the phase shifts are designed to be the same, so that the reflected signal by these elements can add up in-phase at the receiver and maximum gain can be achieved. Then the expression of equivalent channel is simplified to the Fourier transform of reflective intensity across Fresnel zones modulated by the designed phase. Based on this relationship, we prove that the uniformly distributed in-band gain with aligned phase along the Fresnel zone leads to the upper bound of achievable rate, where the gain loss on edge frequencies caused by beam split disappears. Finally, we design phase shifts of RIS to approach the upper bound by adopting the stationary phase method. Simulation results confirm the effectiveness of the proposed Fresnel zone-based method in mitigating the near-field beam split effect.

II. SYSTEM MODEL

We consider a RIS-enabled wireless communication system, as shown in Fig. 1. The carrier frequency, bandwidth and number of carriers are denoted as f_c , B, M, respectively. The frequency of k - th subcarrier is expressed as $f_k =$ $f_c + B(\frac{2k-1}{2K} - 1/2)$, for k = 1, ..., K. We consider a square RIS array with a side length of D. The RIS lies in the xyplane centering at the origin (0,0,0) and the edges of RIS are parallel to the axes respectively. The RIS has $N_1^{\rm RIS}$ and $N_2^{\rm RIS}$ elements on x and y axis respectively, with a total number of $N^{\rm RIS} = N_1^{\rm RIS} N_2^{\rm RIS}$. The space between successive elements along the x and y dimensions is d. The set of 3D coordinates of element of RIS is defined as \mathcal{S} . The coordinate of RIS element (n_x,n_y) is $\mathbf{r}_n^{\mathrm{RIS}}=((n_x-\frac{N_1^{\mathrm{RIS}}+1}{2})d,(n_y-\frac{N_2^{\mathrm{RIS}}+1}{2})d,0)$, where the index of element n is defined as $n=(n_x-1)N_2^{\mathrm{RIS}}+n_y$. The base station (BS) located at $\mathbf{r}^{BS} = (x^{BS}, y^{BS}, z^{BS})$ is assumed to be with $N^{\rm BS}=N_1^{\rm BS}N_2^{\rm BS}$ antennas with $N_1^{\rm BS}$ and $N_2^{\rm BS}$ in the direction ${\bf u_1}$ and ${\bf u_2}$ respectively. The location of BS antenna (n_1,n_2) is ${\bf r}_n^{\rm BS}={\bf r}^{\rm BS}+n_1{\bf u_1}+n_2{\bf u_2}$, where the index of element n is defined as $n = (n_1 - 1)N_2^{BS} + n_2$. A single receiver (UE) is considered with the location at ${\bf r}^{\rm UE} = (x^{\rm UE}, y^{\rm UE}, z^{\rm UE})$. Then the distance from n-th RIS element at \mathbf{r}_n to UE and m-th element of BS can be expressed as $l_n^{\text{R-U}} = \|\mathbf{r}_n - \mathbf{r}^{\text{UE}}\|_2$ and $l_{n,m}^{\text{B-R}} = \|\mathbf{r}_n - \mathbf{r}_m^{\text{BS}}\|_2$ respectively. Furthermore, $R^{\text{B-R}} = \|\mathbf{r}^{\text{BS}}\|_2$ and $R^{\text{R-U}} = \|\mathbf{r}^{\text{UE}}\|_2$ are defined as the central distance.

In this paper, the BS-UE LOS channel is assumpted to be blocked. As the gains of NLOS channels are usually negligible in mmWave/THz band, only the BS-RIS and RIS-UE LOS

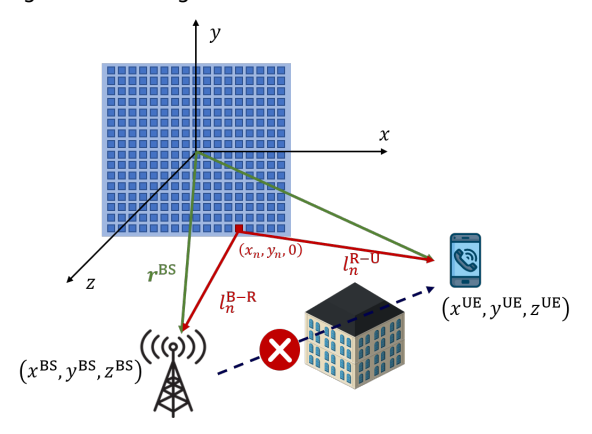


Fig. 1. System model.

channels are considered. The received signal of the k-thsubcarrier can be expressed as

$$y_k = \left(\mathbf{h}_k^{\text{R-U}}\right)^T \mathbf{\Theta} \mathbf{H}_k^{\text{B-R}} \mathbf{v}_k x_k + n_k, \tag{1}$$

where, $x_k \in \mathbb{C}$ is the transmitted signal from the BS with power of s, and $n \sim \mathcal{CN}(0, \sigma_n^2)$ is the additive write Gaussian noise. The RIS elements are assumed to follow the constant reflection amplitude constraint [14] and the reflection coefficient matrix can be written as $\Theta = \operatorname{diag}(\mathbf{w})$, where $\mathbf{w} =$ $[e^{j\phi_1},\ldots,e^{j\phi(x_n)}]$. As the near-field LOS channel model are considered [7], the entries of RIS-UE channel vector $\mathbf{h}_k^{\text{R-U}}$ \in $\mathbb{C}^{N^{\mathrm{RIS}} \times 1}$ and BS-RIS channel matrix $\mathbf{H}_{l}^{\mathrm{B-R}} \in \mathbb{C}^{N^{\mathrm{RIS}} \times N^{\mathrm{BS}}}$ can be written as

$$[\mathbf{h}_{k}^{\text{R-U}}]_{n} = \frac{c}{2\pi f_{k} l_{n}^{\text{R-U}}} e^{-j2\pi f_{k} l_{n}^{\text{R-U}}/c}$$
 (2a)

$$\begin{split} \left[\mathbf{h}_{k}^{\text{R-U}}\right]_{n} &= \frac{c}{2\pi f_{k} l_{n}^{\text{R-U}}} e^{-j2\pi f_{k} l_{n}^{\text{R-U}}/c} \\ \left[\mathbf{H}_{k}^{\text{B-R}}\right]_{(n,m)} &= \frac{c}{2\pi f_{k} l_{n,m}^{\text{B-R}} \sqrt{N^{\text{BS}}}} e^{-j2\pi f_{k} l_{n,m}^{\text{B-R}}/c}. \end{split} \tag{2a}$$

Here we assume the array size of BS is relative small compared with RIS, due to the high hardware cost of BS antenna system. The far-field assumption is adopted in such a small aperture. In this assumption, distance term $l_{n,m}^{\text{B-R}}$ in (2b) is approximated by $l_{n,m}^{\text{B-R}} = \|\mathbf{r}_n^{\text{B-R}} - (\mathbf{r}_{n,m}^{\text{B-R}} - \mathbf{r}^{\text{BS}})\|_2 \approx l_n^{\text{B-R}} - \xi_1 m_1 d - \xi_2 m_2 d$, where $l_n^{\text{B-R}}$ is the distance from the center of BS to n-th RIS element, ξ_1 and ξ_2 are the anglesof-departure (AoD) at BS side and m is decomposed to $m = (m_1 - 1)N_2^{BS} + m_2$. Then the BS-RIS channel matrix can be rewritten as

$$\mathbf{H}_{k}^{\text{B-R}} = \mathbf{h}_{k}^{\text{B-R}} \left(\mathbf{h}_{k}^{\text{BS}} \right)^{T}, \tag{3}$$

where $\mathbf{h}_k^{\text{B-R}}$ is the near-field array response at RIS with $\left[\mathbf{h}_k^{\text{B-R}}\right]_n = \frac{c}{2\pi f l_n^{\text{B-R}}} e^{-j2\pi f_k l_n^{\text{B-R}}/c}$ and \mathbf{h}_k^{BS} is the far-field array response at BS with $\left[\mathbf{h}_k^{\text{BS}}\right]_m = \frac{1}{\sqrt{N^{\text{BS}}}} e^{j2\pi f_k d(\xi_1 m_1 + \xi_2 m_2)/c}$. Then the system model can be written as

$$y_k = \mathbf{w}^T \mathbf{h}_k^{\mathrm{C}} \left(\mathbf{h}_k^{\mathrm{BS}} \right)^T \mathbf{v}_k x_k + n_k, \tag{4}$$

where $\mathbf{h}_k^{ ext{C}} = \mathbf{h}_k^{ ext{R-U}} \odot \mathbf{h}_k^{ ext{B-R}}$ denotes the cascaded channel of RIS. As our work is focused on the beamforming of RIS, the beamforming of BS is assumed to be ideal, i.e. $\mathbf{v}_k = (\mathbf{h}_k^{\text{BS}})^*$. Then the equivalent channel from the BS to the UE can be expressed as

$$g_k = \mathbf{w}^T \mathbf{h}_k^{\mathsf{C}} \left(\mathbf{h}_k^{\mathsf{BS}} \right)^T \mathbf{v}_k = \sqrt{N^{\mathsf{BS}}} \mathbf{w}^T \mathbf{h}_k^{\mathsf{C}}. \tag{5}$$

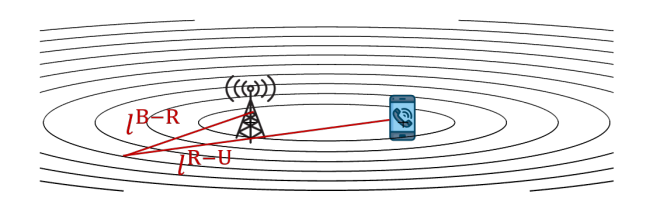


Fig. 2. A series of Fresnel zones of the communication system with a BS and a UE. The transmission length $l^{\rm B-R}+l^{\rm R-U}$ remains the same on each Fresnel zone.

III. FRESNEL ZONE MODEL FOR RIS CHANNEL

The equivalent channel g_k in (5) is the summation of subchannels via elements over the 2-dimensional RIS plane with non-linear phase terms due to distance, making beamforming design complex. In this section, the concept of Fresnel zone is introduced to deal with the RIS cascaded channel. Then we will show that RIS elements on a single Fresnel zone will not suffer from beam split effect, followed by a coordinate transformation which can reduce the problem to a 1-dimensional integration across Fresnel zones with linear phase term.

A. Introduction to the Fresnel Zone

In the context of radio propagation, Fresnel zones refer to the concentric ellipsoids whose foci are the transmitter and receiver. The property of ellipsoids ensures that the signals reflected by RIS elements on the same Fresnel zone have the same route length $l = l^{\text{B-R}} + l^{\text{R-U}}$, as shown in Fig. 2.

The intersections of ellipsoids of Fresnel zones and the RIS plane are a series of ellipses. It's hard to determine correspondence between the RIS elements and the Fresnel zones, due to mismatch of continuous-shaped Fresnel zones and the discrete spacing of RIS. To address this, we use an imaginary continuous RIS (I-RIS) to approximate the RIS with discrete spacing. The I-RIS contains an uncountable number of virtual elements lying in the set $S_C = \{(x,y)||x| < a\}$ D/2, |y| < D/2. The overall reflection gain of the virtual elements within the area of an original RIS element should equal the gain of that RIS element. Therefore, the weight of the virtual element located at (x, y, 0) is normalized to $w(x,y) = e^{j\phi(x,y)}/d^2$. As the elements of the discrete RIS can be regarded as spatial sampling of continuous I-RIS, the accuracy of the approximation can be ensured by the Nyquist spatial sampling theorem. Similar to the expression in (5), the equivalent channel for I-RIS system is expressed as

$$g(f) = g_0 \int_{-\frac{D}{2}}^{\frac{D}{2}} \int_{-\frac{D}{2}}^{\frac{D}{2}} e^{j\phi - j2\pi f(l^{\text{B-R}} + l^{\text{R-U}})/c} dx dy,$$
 (6)

where $g_0 = \frac{\sqrt{N^{\rm BS}}c^2}{4\pi^2f^2R^{\rm B-B}R^{\rm R-U}d^2}$ is the basic path-loss. Here we write the equivalent channel g(f) as a function of frequency to simplify presentation.

The idea of continuous spacing I-RIS is just a mathematical technique to aid the analysis and beamforming design as it can fit the continuity of Fresnel zones. Our subsequent analysis and phase design for the I-RIS closely approximate the discrete RIS, and the phase design will be applied at the locations of the discrete RIS elements

The reason that we introduce the Fresnel zone is that the beam split effect disappears when only virtual I-RIS elements on one Fresnel zone are considered. Specifically, subchannels via elements on the Fresnel zone have aligned phase $-2\pi f l/c$ as they share same route length l, ensuing an inphase combination of signal at the receiver. As the phase of these elements is designed to be the same, the gain keeps maximized and the beam keeps focused to the UE's location regardless of frequency. Therefore, elements along one Fresnel zone do not suffer from beam split effect. When more Fresnel zones are considered, the signal reflected by elements on different Fresnel zones cannot keep aligned phase as frequency changes, resulting in the gain loss. In other words, the beam split effect only occurs across the Fresnel zones. Therefore, our design can focus only on addressing the beam split across different Fresnel zones, instead of the whole RIS plane.

B. Coordinate transformation based on Fresnel zone

In this subsection, we transform the Cartesian coordinate into the proposed Fresnel-zone coordinate with dimensions that are along and across the Fresnel zones on the I-RIS plane.

The Fresnel zones of the system are a set of concentric ellipsoids whose foci are the transmitter and receiver. The semimajor axis length of the ellipsoid is defined as a. According to the property of ellipsoids, the length of reflecting route is $l=l^{\rm B-R}+l^{\rm R-U}=2a$. Besides, the intersection of the Fresnel zone and the plane z=0 where the RIS is located is an ellipse, which has a function of

$$\sqrt{(x^{\text{BS}} - x)^2 + (y^{\text{BS}} - y)^2 + z^{\text{BS}^2}} + \sqrt{(x^{\text{UE}} - x)^2 + (y^{\text{UE}} - y)^2 + z^{\text{UE}^2}} = 2a.$$
 (7)

In order to simplify the subsequent process, coordinate translation and rotation are adopted so that the two roots in (7) have symmetry format. Specifically, we establish a new Cartesian coordinate system. The origin is the projection of the midpoint $(x_c,y_c)=(\frac{x^{\rm BS}+x^{\rm UE}}{2},y_c=\frac{y^{\rm BS}+y^{\rm UE}}{2})$ of the transmitter receiver connection on the RIS plane and the x-axis direction is set as the direction of the transmitter pointing to the receiver. The coordinate translation can be written as

$$\begin{cases} x' = (x - x_c)\cos\alpha + (y - y_c)\sin\alpha\\ y' = -(x - x_c)\sin\alpha + (y - y_c)\cos\alpha, \end{cases}$$
(8)

where $\alpha = \arctan \frac{y^{\rm BS} - y^{\rm UE}}{x^{\rm BS} - x^{\rm UE}}$ is the angle of rotation. Then the ellipse in (7) can be expressed as

$$\sqrt{(x'+u)^2 + y'^2 + z^{BS^2}} + \sqrt{(x'-u)^2 + y'^2 + z^{UE^2}} = 2a,$$
(9)

where $u=\frac{1}{2}\sqrt{(x^{\rm BS}-x^{\rm UE})^2+(y^{\rm BS}-y^{\rm UE})^2}$ is half of the projection length of transmission route to the plane of RIS, and $b=\sqrt{a^2-u^2}$. (9) is not the standard form of a ellipse,

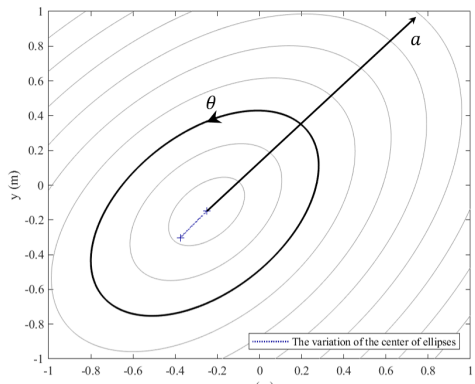


Fig. 3. The intersections of Fresnel zones and the RIS plane are a series of ellipses. A new coordinate system is set on the ellipses with axes of semi-major axis a of Fresnel zone and angular coordinate θ .

making it hard to analyze its properties. So we rewrite it into the standard form

$$\frac{(x'-x_0)^2}{a^2k_0^2} + \frac{y'^2}{b^2k_0^2} = 1, (10)$$

where $x_0 = \frac{1}{4}u\frac{z^{\mathrm{BS}}s^2 - z^{\mathrm{UE}2}}{(a^2 - u^2)^2}$ is the center of the ellipse, and $k_0 = \sqrt{1 + \frac{\left(z^{\mathrm{UE}^2} - z^{\mathrm{BS}^2}\right)^2}{16b^4} - \frac{1}{2}\frac{z^{\mathrm{BS}^2} + z^{\mathrm{UE}^2}}{b^2}}$ is the correction factor for the semi-major axis and the semi-minor axis, and the length of both semi-major and semi-minor axes become k times of the original. The series of ellipses are depicted in Fig. 3.

In classical polar coordinate system, the Cartesian coordinates x and y can be converted to the radial coordinate r and the angular coordinate θ . In the Fresnel zone system, we use the length of semi-major axis a to replace the radial coordinate r, while the angular coordinate θ remains the same meaning, as shown in Fig. 3. Then the transformation of coordinate can be expressed by using the trigonometric functions

$$\begin{cases} x' = ak_0 \cos \theta + x_0 \\ y' = \sqrt{a^2 - u^2} k_0 \sin \theta. \end{cases}$$
 (11)

After the transformation of coordinate, the point set of RIS elements changes from \mathcal{S}_C to $\mathcal{V}_0 = \{(a,\theta)|\ (x(a,\theta),y(a,\theta),0)\in\mathcal{S}_C\}$, where $x(a,\theta)$ and $y(a,\theta)$ are the original Cartesian coordinates of the point (a,θ) in the Fresnel zone coordinate. Then the equivalent channel can be rewritten as

$$g(f) = \int_{a} e^{-j2\pi f \frac{2a}{c}} \int_{\theta} g_0 e^{j\phi(a,\theta)} J(a,\theta) d\theta da, \qquad (12)$$

where $J(a,\theta) = \left| \frac{\partial (x',y')}{\partial (a,\theta)} \right|$ is the absolute value of the Jacobian of the transformation. Note that the inner integral along the Fresnel zone in (12) is frequency independent. So the beam split effect will not occur when the I-RIS elements on same Fresnel zone are considered. The phase $\phi(a,\theta)$ is designed to be the same along the Fresnel zone with semi-major length a, i.e. $\phi(a,\theta) = \psi(a)$, so that the reflective intensity of each Fresnel zone can always reach its maximum value.

The inner integral then becomes a real value integral of the Jacobian

$$v(a) = \int_{\theta \in \mathcal{V}(a)} g_0 J(a, \theta) d\theta, \tag{13}$$

where $\mathcal{V}(a) = \{\theta | (a,\theta) \in \mathcal{V}_0\}$ is the set of angle of point which lies in the region of RIS. The value of integral v(a) is regarded as the reflective intensity of Fresnel zone with semi-major length a. With the aligned phase design along the Fresnel, the equivalent channel can be rewritten as

$$g(f) = \int_{a} v(a)e^{j\psi(a)}e^{-j2\pi f\frac{2a}{c}}da.$$
 (14)

Here we get a one-dimensional integral across the Fresnel zones, with phase term $-j2\pi f\frac{2a}{c}$ linear to the integral variable a. Further, the integral across the Fresnel zones can be transformed to a Fourier transform. If we use transmit delay t=2a/c to replace a, the integral becomes

$$g(f) = \int_{t} v_t(t)e^{j\psi_t(t)}e^{-j2\pi ft}dt, \qquad (15)$$

where we use $v_t(t) = \frac{c}{2}v\left(t\frac{c}{2}\right)$ and $\psi_t(t) = \psi\left(t\frac{c}{2}\right)$ to simplify writing, without change of their physical meaning. Therefore, the equivalent channel g(f) is the Fourier transform of Fresnel zone intensity $v_t(t)$ modulated by phase design $\psi_t(t)$.

IV. UPPER BOUND OF ACHIEVABLE RATE IN WIDEBAND RIS SYSTEM

In this section, an upper bound of achievable rate is proposed for wideband RIS-enabled system. The result shows that the upper bound is reached when the channel gain distributes evenly in-band without out-of-band leakage.

Here, the number of subcarriers is assumed to be infinite. This assumption renders the result general, as any subcarrier configuration can be seen as sampling of the continuous frequency band. The achievable rate can be written as

$$R = \int_{f_c - B/2}^{f_c + B/2} \log_2 \left(1 + \frac{|g(f)|^2 S_x}{S_\sigma} \right) df, \qquad (16)$$

where S_x is the energy of signal and S_{σ} is the power spectrum density of noise.

The achievable rate is bounded by

$$\int_{f_{c}-\frac{B}{2}}^{f_{c}+\frac{B}{2}} \log_{2}\left(1 + \frac{|g(f)|^{2} S_{x}}{S_{\sigma}}\right) df$$

$$\stackrel{(a)}{\leq} B \log_{2}\left(1 + \frac{S_{x}}{S_{\sigma}} \int_{f_{c}-\frac{B}{2}}^{f_{c}+\frac{B}{2}} |g(f)|^{2} df\right)$$

$$\stackrel{(b)}{\leq} B \log_{2}\left(1 + \frac{S_{x}}{S_{\sigma}} \int_{-\infty}^{+\infty} |g(f)|^{2} df\right)$$

$$\stackrel{(c)}{=} B \log_{2}\left(1 + \frac{S_{x}}{S_{\sigma}} \int_{t}^{t} v_{t}^{2}(t) dt\right),$$

$$(17)$$

where (a) holds due to the Jensen's inequality and (c) is based on the Fourier transform relationship between g(f) and $v_t(t)e^{j\psi_t(t)}$ in (15) and the Parseval's theorem. Here, $E_g=\int_t v_t^2(t)\mathrm{d}t$ is considered as the energy of channel, which

is maximized since $v_t(t)$ is at its highest reflective intensity along the Fresnel zone. Therefore, $B\log_2\left(1+\frac{S_x}{S_\sigma}E_g\right)$ is the upper bound of achievable rate for phase configuration of the I-RIS in LOS scenario.

Additionally, we analyze the condition for the achievable rate to reach its upper bound. The equality in (a) is attained when $|g(f)|^2$ remains constant in the frequency band $[f_c-B/2,f_c+B/2]$ and the equality in (b) is achieved when no gain leaks out of the frequency band, i.e. $g(f)=0, f\in (-\infty,f_c-B/2)\cup (f_c+B/2,+\infty)$. Therefore, the ideal gain spectrum to reach the upper bound can be written as

$$\hat{g}(f) = \begin{cases} \sqrt{\frac{E_g}{B}} & f \in [f_c - B/2, f_c + B/2] \\ 0 & \text{otherwise.} \end{cases}$$
 (18)

Note that the upper bound proposed here is suitable for the continuous I-RIS with infinite number of subcarriers. Real systems with discrete spacing RIS and finite number of subcarriers can be seen as the sampling in both space and frequency domain. The proposed upper bound and ideal condition are still valid in real systems, as no additional benefit in rate can be obtained through the sampling procedure. Besides, the ideal gain is not reachable, because the band-limited spectrum of gain can not be formed by a time-limited signal $v_t(t)e^{j\psi_t(t)}$. In the next section, we will propose phase design for $\psi_t(t)$ to approach the ideal gain spectrum.

Algorithm 1: Near-field Wideband RIS Beamforming Based on Fresnel Zones

Inputs: The location of BS $(x^{\text{BS}}, y^{\text{BS}}, z^{\text{BS}})$ and UE $(x^{\text{UE}}, y^{\text{UE}}, z^{\text{UE}})$; designed bandwidth B; center frequency f_c

- 1. Translate the coordinate system by (8).
- 2. Determine the semi-major axis a of Fresnel zones with proper division in $[a_{\min}, a_{\max}]$, and calculate inner integral v(a) by (13).
- 3. Obtain phase design across Fresnel zones $\psi(a)$ by (19).
- 4. Calculate phase shift ϕ_n by (20) for $n = 1, ..., N^{RIS}$. **Outputs:** The phase shift matrix $\Theta = \text{diag}(\phi_1, ..., \phi_n)$.

V. WIDEBAND BEAMFORMING BASED ON FRESNEL ZONE

In this section, Fresnel-zone-based near-field wideband beamforming is proposed to approach the ideal gain and mitigate the loss caused by near-field beam split.

Specifically, we propose phase design for $\psi_t(t)$ in (15) to approach the ideal spectrum $\hat{g}(f)$ in (18) which can reach the upper bound of achievable rate. Recall that in (15), g(f) is the Fourier transform of a phase-modulated wave $v_t(t)e^{j\psi_t(t)}$, where the intensity $v_t(t)$ is fixed and $\psi_t(t)$ is the modulating phase to be designed. Stationary phase method is a widely used approach for phase-modulated signal design in the field of radar, which can be adopted to approach the desired spectrum [15]. Based on the stationary phase method, we provide a

nearly closed-form expression of the design of phase shifts on Fresnel zones,

$$\psi(a) = \frac{4\pi B}{c} \frac{\int_{a_{\min}}^{a} \int_{a_{\min}}^{a_{1}} v^{2}(a_{2}) da_{2} da_{1}}{\int_{a_{\min}}^{a_{\max}} v^{2}(a_{2}) da_{2}} + \frac{4\pi a \left(f_{c} - \frac{B}{2}\right)}{c}. (19)$$

Finally, the phase of each RIS element can be calculated. The phase shift configuration of each RIS element takes the value of the designed phase of the Fresnel zone which it belongs to, i.e.

$$\phi_n = \psi\left(\frac{l_n^{\text{B-R}} + l_n^{\text{R-U}}}{2}\right). \tag{20}$$

In practice, the integral for calculating v and $\psi(a)$ is realized through numerical integration, with the integration interval $[a_{\min}, a_{\max}]$ properly divided. This division can work effectively when the interval between two integral points is less than half the spacing of the RIS elements.

The algorithm of near-field wideband beamforming based on Fresnel zone is summarized in **Algorithm 1**. The algorithm exhibits low complexity, as the computational complexity is not greater than $O(N^{\rm RIS})$ in each step.

VI. SIMULATION RESULTS

In this section, simulation results are provided to validate the effectiveness of the proposed wideband beamforming method based on Fresnel zone.

We consider a near-field system with a square planar RIS of side length $D=1\mathrm{m}$. The TX is located in $(5.6\mathrm{m},5\mathrm{m},12.6\mathrm{m})$ and the RX is located in $(-4.2\mathrm{m},5\mathrm{m},5.6\mathrm{m})$. The carrier frequency f_c is set as 30GHz. We use half-wavelength spacing of the RIS elements. The bandwidth is set to $B=2.5\mathrm{GHz}$ with K=256 subcarriers. It is assumed that the location of the TX and the RX, equivalently the channel $\mathbf{H}_k^{\mathrm{B-R}}$ and $\mathbf{h}_k^{\mathrm{R-U}}$ are known at the RIS controller.

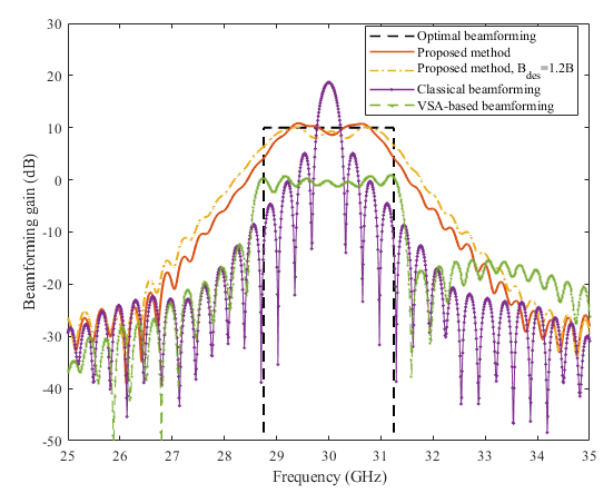


Fig. 4. Beamforming gain at different frequencies.

The beamforming gain at different frequencies is shown in Fig. 4. It can be observed that the beamforming gain is approximately flat over the frequency band, close to the optimal gain spectrum in (18). Compared with the classical narrow band beamforming, the proposed method can mitigate

losses at the edge frequencies and overcome the near-field beam split effect. Besides, although the VSA-based method [12] can also achieve a flat in-band gain, the gain is low due to the separate design of subarrays. Note that about 3dB loss still exists for the proposed method at the very edge of the frequency band. One can choose a wider bandwidth $B_{\rm des}=1.2B$ for beamforming design as shown in Fig. 4. This adjustment can increase the gain at edge frequencies, but at the expense of lower in-band gain and higher out-of-band leakage. A trade-off to determine the value of $B_{\rm des}$ can be made in practice.

Next, we provide the simulation results for average achievable rate. In each random experiment, the TX and the RX are randomly located in the distance range [7m, 13m]. We investigate the average achievable rate as a function of transmit power, as shown in Fig. 5. The proposed method exhibits a 50% increase in achievable rate compared to the classical beamforming and a 30% increase compared to the VSA-based beamforming [12], while maintaining a marginal deficit of less than 5% relative to the optimal benchmark. Furthermore, employing solely 2-bit phase shifters, the proposed method almost approaches the performance of continuous phase shifters, despite its lower hardware complexity and cost.

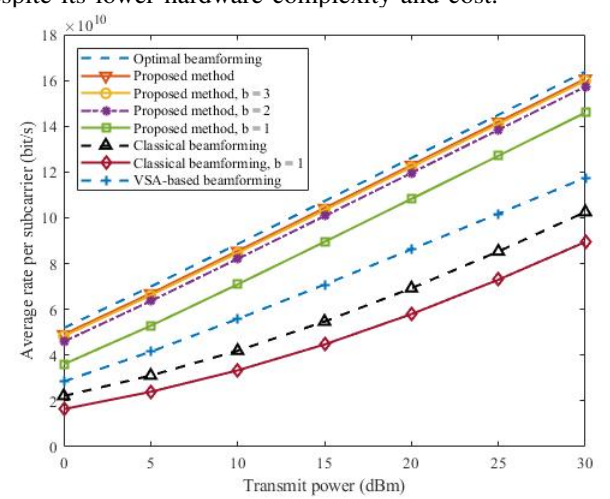


Fig. 5. Simulation results of average achievable rate vs. transmit power.

VII. CONCLUSION

In this work, we have addressed the near-field beam split effect in RIS-aided wideband communications, a critical issue that leads to significant beamforming gain loss. To tackle this problem, we propose a novel near-field wideband RIS beamforming method based on Fresnel zones, representing the first introduction of the principle of Fresnel zones from electromagnetic measurement into RIS communications. This approach offers a fresh perspective for RIS beamforming, leveraging the inherent properties of Fresnel zones to enhance the performance of wireless communication systems. Through simulations, we demonstrated that our method can effectively mitigate the near-field beam split effect, resulting in a nearly flat gain across the entire frequency band. This was achieved without increasing the hardware complexity or cost, which is suitable for practical implementation in RIS systems.

VIII. ACKNOWLEDGMENT

This work was supported in part by the National Science Fund for Distinguished Young Scholars (Grant No. 62325106), in part by the National Key R&D Program of china (No.2023YFB811503), and in part by ZTE Industry-University-Institute Cooperation Funds under Grant No. HC-CN-20200923014.

REFERENCES

- [1] Z. Chen, C. Han, Y. Wu, L. Li, C. Huang, Z. Zhang, G. Wang, and W. Tong, "Terahertz wireless communications for 2030 and beyond: A cutting-edge frontier," *IEEE Communications Magazine*, vol. 59, no. 11, pp. 66–72, 2021.
- [2] R. Wei, Q. Xue, S. Ma, Y. Xu, L. Yan, and X. Fang, "Joint optimization of active and passive beamforming in multi-IRS aided mmWave communications," in 2022 IEEE Globecom Workshops (GC Wkshps). IEEE, 2022, pp. 136–141.
- [3] C. Desset, P. Wambacq, Y. Zhang, M. Ingels, and A. Bourdoux, "A flexible power model for mm-wave and THz high-throughput communication systems," in 2020 IEEE 31st Annual International Symposium on Personal, Indoor and Mobile Radio Communications, 2020, pp. 1–6.
- [4] M. Cui, Z. Wu, Y. Chen, S. Xu, F. Yang, and L. Dai, "Demo: Low-power communications based on RIS and AI for 6G," in *Proc. IEEE ICC*, 2022.
- [5] X. Li, H. Lu, Y. Zeng, S. Jin, and R. Zhang, "Modular extremely large-scale array communication: Near-field modelling and performance analysis," *China Communications*, vol. 20, no. 4, pp. 132–152, 2023.
- [6] M. Cui and L. Dai, "Near-field wideband beamforming for extremely large antenna arrays," arXiv preprint arXiv:2109.10054, 2021.
- [7] M. Cui, Z. Wu, Y. Lu, X. Wei, and L. Dai, "Near-Field MIMO Communications for 6G: Fundamentals, Challenges, Potentials, and Future Directions," *IEEE Communications Magazine*, vol. 61, no. 1, pp. 40–46, 2023.
- [8] N. J. Myers and R. W. Heath, "InFocus: A Spatial Coding Technique to Mitigate Misfocus in Near-Field LoS Beamforming," *IEEE Transactions* on Wireless Communications, vol. 21, no. 4, pp. 2193–2209, 2022.
- [9] W. Hao, X. You, F. Zhou, Z. Chu, G. Sun, and P. Xiao, "The Far-/Near-Field Beam Squint and Solutions for THz Intelligent Reflecting Surface Communications," *IEEE Trans. Veh. Technol.*, vol. 72, no. 8, pp. 10107–10118, Aug. 2023.
- [10] J. Wang, J. Xiao, Y. Zou, W. Xie, and Y. Liu, "Wideband Beamforming for RIS Assisted Near-Field Communications," arXiv preprint arXiv:2401.11141, 2024.
- [11] B. Govind, T. Tapen, and A. Apsel, "Ultra-compact quasi-true time delay for boosting wireless channel capacity," *Nature*, vol. 627, no. 8002, pp. 88–94, Mar. 2024.
- [12] Y. Cheng, C. Huang, W. Peng, M. Debbah, L. Hanzo, and C. Yuen, "Achievable Rate Optimization of the RIS-Aided Near-Field Wideband Uplink," *IEEE Trans. Wireless Commun.*, vol. 23, no. 3, pp. 2296–2311, Mar. 2024.
- [13] Q. Wu and R. Zhang, "Towards Smart and Reconfigurable Environment: Intelligent Reflecting Surface Aided Wireless Network," *IEEE Communications Magazine*, vol. 58, no. 1, pp. 106–112, 2020.
- [14] L. Dai, B. Wang, M. Wang, X. Yang, J. Tan, S. Bi, S. Xu, F. Yang, Z. Chen, M. D. Renzo, C.-B. Chae, and L. Hanzo, "Reconfigurable Intelligent Surface-Based Wireless Communications: Antenna Design, Prototyping, and Experimental Results," *IEEE Access*, vol. 8, pp. 45 913–45 923, 2020.
- [15] C. Cook, Radar signals: An introduction to theory and application. Elsevier, 2012.